

Final Report

NEEDLE LOCALIZATION IN CT-GUIDED TUMOR ABLATION

EN 601.456 Computer Integrated Surgery II

Giang Hoang
giang@jhu.edu
B.S - M.S.E Biomedical Engineering Student, Johns Hopkins University

Table of Contents

Project Statement	3
Introduction	3
1. Clinical Motivation	3
2. Prior Work	4
2A. Prior work in ablation needle localization	4
2B. Prior work in needle detection in 3D ultrasound images	4
3. Goals	5
4. Overall Integration Into The Workflow	5
Technical Approach	6
1. Needle Segmentation and Feature Extraction With MATLAB	6
1A. Preprocessing	6
1B. Connected Component Analysis and Object Filtering	7
1C. Feature Extraction: Needle Orientation and Tip Location	7
2. Ablation Zone Approximation Using Ellipsoidal Model	8
Evaluation and Experimental Setup	9
1. Needle segmentation algorithm evaluation using medical images	9
2. Ablation zone prediction demonstration with thermochromic phantom and ex vivo experiments	9
2A. Tissue-mimicking Thermochromic Phantom	9
2B. Ex vivo Bovine Liver	10
Results	10
1. Algorithm Performance With Medical Images	10
2. Ablation Zone Evaluation With Tissue-mimicking Thermochromic Phantom	11
3. Preliminary Integration of Ablation Zone Prediction Into Tumor Ablation Procedure	12
Discussion	14
Progress Evaluation	14
1. Dependencies	14
2. Key Activities and Deliverables	15
3. Schedule Adherence	16
Final Remarks	16
References	17
Appendix 1: Code Documentation	18

Project Statement

This project aims to develop an algorithm to localize and identify the orientation of the ablation needle to predict the ablation zone during a minimally-invasive tumor ablation procedure.

Introduction

1. Clinical Motivation

Radiofrequency Ablation or Microwave Ablation are minimally invasive surgical procedures that utilize the heat generated from electrical energy to destroy cancer cells [1]. The procedure is commonly used to treat small tumors, especially in areas that are close to important anatomical structures (**Figure 1**) [2]. Tumor ablation involves inserting a needle that allows the passage of high-frequency energy, which heats up a targeted area in the tumor and induces coagulative necrosis. The efficacy of the treatment is affected by the impedance and heat regulation of the tissue and most importantly, the location of the ablation needles with respect to the tumor [3]. Thus, it is highly dependent on image guidance to help physicians accurately insert the needles to the ablation site. However, over-treated and under-treated tumors are very common. A 2009 report on liver tumor ablation with RFA showed 9% of cases have major complications from overtreatment and around 40% of cases had undertreated tumors that may result in recurrence [3]. This urges for current image guidance practice to be enhanced in order to improve clinical outcomes of tumor ablation.

Due to the advantageous minimal invasiveness and shorter period of recovery associated ablation procedure, researchers from the Nation Institute of Health (NIH) Clinical Centers are actively working on integrating and optimizing tumor ablation into the treatment of larger tumors. However, large tumors require the use of multiple ablation needles, each contributing to the overall ablation zone. On most occasions, many ablation needles need to be inserted either concurrently or sequentially to cover the span of the entire tumor. To support this effort, an algorithm was developed to automate the needle identification process in Computed Tomography (CT) images and help physicians better visualize the ablation zone intraoperatively.



Fig 1. Image-guided Tumor Ablation Procedure (images provided by Dr. Sheng Xu, NIH Clinical Center)

2. Prior Work

2A. Prior work in ablation needle localization

There have been multiple attempts to automatically localize needles in tumor ablation procedures. Most notably, the incorporation of electromagnetic (EM) trackers on the ablation needle has resulted in promising outcomes [4, 5]. Specifically, an EM tracker is used to track the ablation needle trajectory and tip location with respect to the preoperative CT scan of the patient (**Figure 2**). While EM tracker can help decrease the dependence on frequent imaging input, the procedure requires an elaborated calibration protocol to relate the EM tracker coordinate system with the CT coordinate system. To obtain high accuracy, the incorporation of EM trackers onto the ablation needle also requires the modification of surgical tools, which poses a barrier to its clinical adoption. Moreover, due to the use of preoperative CT scan, no information regarding tissue movement is presented, thus providing physicians with real-time needle trajectory with respect to a static non-real-time surgical site. Despite its barriers, this work provides an important clinical interface for the adoption of new needle localization methods into the current workflow.

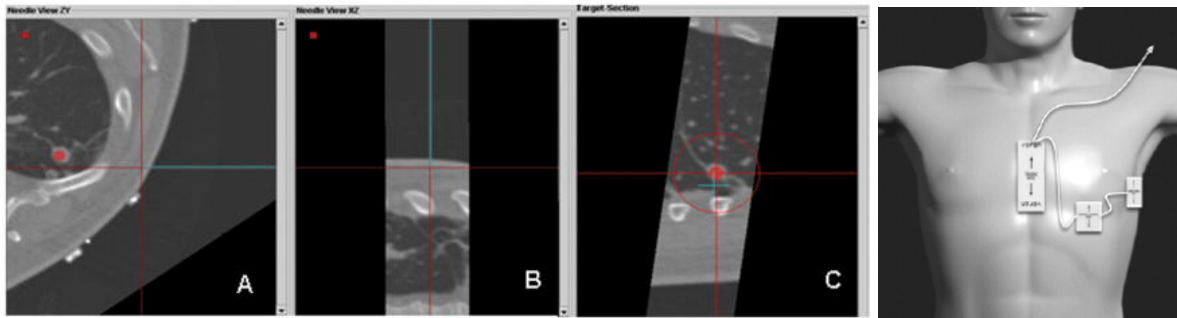


Fig 2. (A-C) Ablation needles tracked by EM with custom tracking software [5]; (D) EM tracker pads are placed on the patient's chest and an EM generator is mobile which can be placed on the patient's skin [4].

2B. Prior work in needle detection in 3D ultrasound images

Several needle localization algorithms have been developed for 3D Ultrasound images and have been proven to be effective [6, 7]. A popular algorithm is the 3D Hough transform, which can be used to determine the location and orientation of a line segment by working with a polar coordinate representation of a line in 3D (**Figure 3**). A 3D modified Hough transforms algorithm was previously developed and showed a less than

2° and 2 mm deviation in angle and location, with a run time of 2 seconds per computation. This is a promising algorithm for application to the current project.

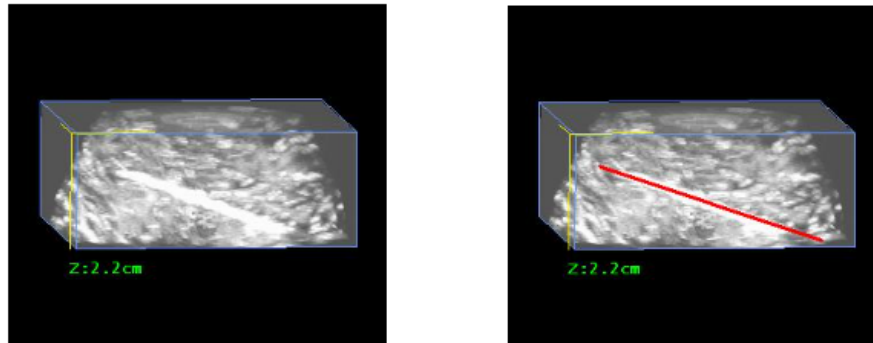


Fig 3. Segmentation of a needle in 3D Ultrasound Image using 3D Improved Hough Transform [6].

3. Goals

This project aims to fully implement a CT image segmentation algorithm to localize the ablation needles intraoperatively. With the information extracted from the location of each needle in the image, an approximate ablation zone will be generated and displayed to serve as guidance for the physician. The algorithm developed is tested on a medical image dataset and evaluated for accuracy and efficiency. Evaluation is also performed on-site with phantom and *ex vivo* samples.

4. Overall Integration Into The Workflow

This section will give a big picture of how the proposed technology fits into the current tumor ablation workflow. The patient is first assessed and screened for the procedure (medical history, pre-op imaging, general health assessment, ...) On the day of the procedure, the patient is first positioned on the procedure/CT table in the operating room and receives anesthetics (locally or intravenously). The physician would then insert the ablation needle with the help of CT image guidance. Each time the physician acquires a CT image, for safety precautions against radiation exposure, they have to leave the operating room and then return to continue the procedure. Once the needle is in place, the physician activates the electrodes that would transmit electrical impulses to ablate the tumor. This process is done until the tumor is completely removed. The incorporation of the needle localization algorithm and ablation zone approximation would be utilized every time a CT image is acquired. This would automatically provide the physician with information such as the current distance and angle between the needle tip with respect to the tumor and other anatomical structures, as well as the approximate coverage of the ablation zone. This not only can support the efficacy of the ablation but may also enable physicians to better evaluate ablations that are close to crucial anatomical structures such as nerves or blood vessels. A diagram of this intervention is shown in **Figure 4**.

For experienced physicians, usually, only one intraoperative CT scan is needed to confirm the correct placement of the ablation needle. Thus, the approximation of the ablation zone given the needle location is of higher interest as compared to needle insertion guidance. By providing an estimation of which part of the tumor is ablated in real-time, the physician can proactively determine the next course of action when using multiple ablation needles, potentially reduce undertreatment and the rate of tumor recurrence.

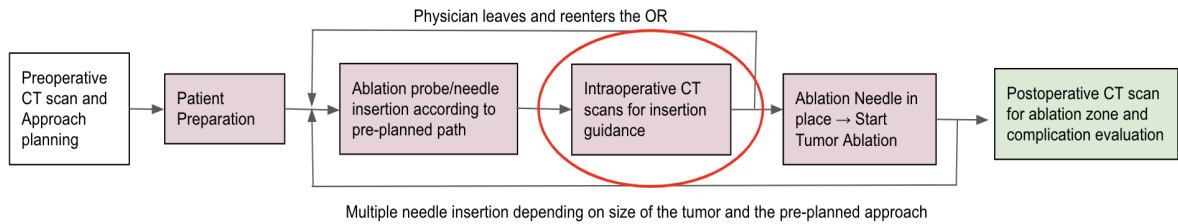


Fig 4. The integration of the project into the tumor ablation procedure workflow

Technical Approach

1. Needle Segmentation and Feature Extraction With MATLAB

This project implements medical imaging analysis algorithms to segment the ablation needles and determines their orientation and tip location using MATLAB. The code documentation and link to the MATLAB source code are attached in **Appendix 1**. A block diagram of the technical approach and the associated image processing result is presented in **Figure 5**.

The input to the algorithm is a Nifti image that is scaled and pan such that the centroid of the body cross-section is relatively close to the center of the image (already standardized for all clinically-acquired CT images). The algorithm also prompts user input to determine whether a single needle or multiple needles are expected.

1A. Preprocessing

Due to the high intensity associated with the metal needles in the CT images, the loaded volume images are standardized to a grayscale 8-bit image and partially thresholded to maintain the true intensity of the selected voxels. The threshold is set such that only the voxels whose intensity lies in the 99.95 percentile of the entire image would be selected. This threshold is optimized through multiple trials to ensure the needle object is maintained. The result of thresholding may include unwanted structures and artifacts.

The volume is then further refined using morphological image reconstruction to fill image holes with 18-connectivity, followed by morphological opening and closing of the volume to remove small artifacts that may interfere with the connected component analysis.

1B. Connected Component Analysis and Object Filtering

The thresholded image is then subjected to connected components analysis using a flood-fill algorithm with 18-connectivity. The connected components are then filtered based on volume, with a lower bound of 30 and an upper bound of 15,000. Volume filter is used to remove small artifacts or larger bone structures.

A shape ratio is also computed for each connected component, which is the ratio between the length of the largest principal axis and the length of the smaller axes (**Equation 1** [7]). The larger this shape ratio, the more elongated and needle-shaped the object is. For images with a single needle, the connected components are selected with a shape ratio greater than 10. To take into account the potential identification of multiple ablation needles as one connected component as they might touch one another, the shape ratio threshold is set to 4 for images with multiple needles. The shape filter is used to remove any remaining bone or metal-like object in the body cavity that was not previously removed by thresholding or volume filtering.

$$\text{Shape Ratio} = \frac{L}{M+S} \quad (\text{Equation 1})$$

L: The length of the largest principal axis of the object

M: The length of the middle principal axis of the object

S: The length of the smallest principal axis of the object

The distance between the centroid of the object with respect to the center of the image is also evaluated to filter out the potential metal wires associated with the ablation procedure that got caught in the CT image but lies further from the center of the body. The threshold for this distance is set to 0.2 times the overall size of the image.

1C. Feature Extraction: Needle Orientation and Tip Location

The connected components representing the needles are now obtained and subjected to feature extraction. The needle orientation is computed using principal component analysis of all of the voxels' locations. The needle tip location is determined by projecting all voxels onto the needle directional axis and obtaining the locations of the two ends of the needle object (minimum and maximum projection values). The needle end that is closer to the center of the body cavity is determined as the needle tip of interest.

For images with multiple needles, 3D Hough Transform Algorithm was applied on the connected components with a shape ratio of less than 10 to separate multiple needles in one connected component. Since 3D Hough Transform is only utilized here to separate different needle objects and high resolution is not needed, the voting space can be smaller to reduce computational time and memory space. Specifically, instead of performing 3D Hough on the entire image space, the Hough space is limited to only the bounding box of the connected component being analyzed. The azimuth and elevation angles are limited to the range $[0^\circ, 90^\circ]$ with an angle increment of 5° . The distance

increment for Hough space varies depending on the size of the bounding box, but the total size of this dimension is fixed to 64. Thus, the resulting size of the Hough space is 18x18x72x64. The algorithm utilized to implement the 3D Hough Transform is detailed in the previously published studies by Zhou et al. [6]. The Hough cells that have more than 300 votes are selected to represent a needle object and all the voxels that voted for those cells are reassembled. Using the reassembled voxels, the direction of the needle fragments is computed using PCA. Fragments with similar orientation (orientation unit vector discrepancy < 0.5) is further clustered using Euclidean linkage to form a needle object. Each needle object is now extracted for direction and tip location in a similar matter described in the previous paragraph.

The needle orientation and tip location of all needles in the image are now obtained and stored in a feature matrix that can be used to generate the ablation zone.

2. Ablation Zone Approximation Using Ellipsoidal Model

Based on technical standards, the volume of the ablation region is approximated using an ellipsoid. The dimensions of the ellipsoid are dependent on the specific ablation needle type, pulse type, ablation duration, and the amount of energy. For example, a Certus^{LK} Single Probe LK15 (MWA) when ablating a bovine liver *ex vivo*, using a 40 W power setting and 5-minute duration, would result in an ellipsoid ablation zone of 3.6 cm (long axis) and 2.6 cm (short axis). With the extracted features, an ellipsoid centered at the needle tip location with a long axis coincides with the needle orientation is generated and overlaid on the thresholded image for visualization.

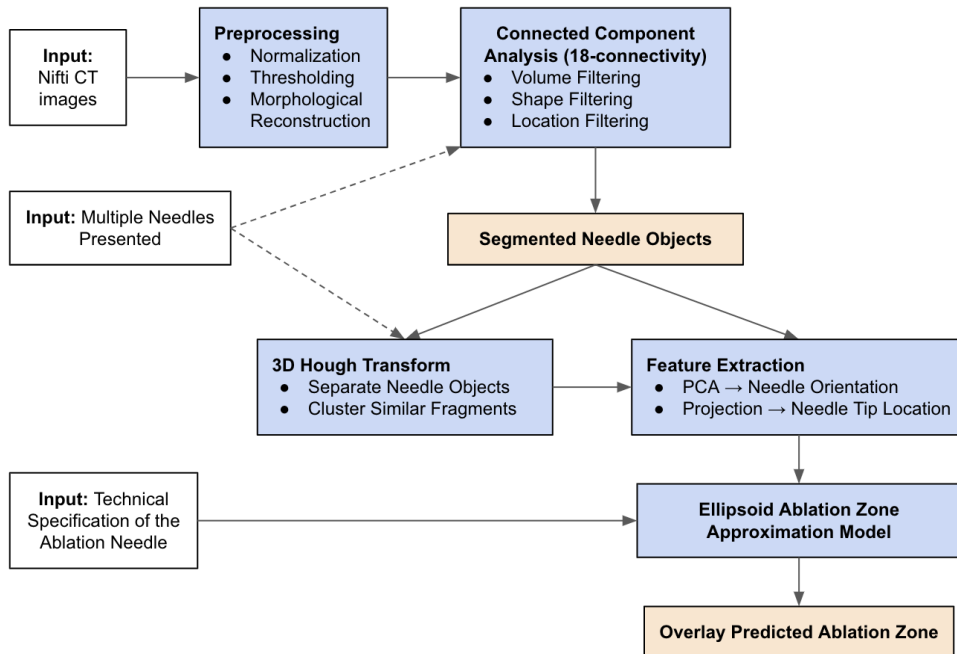


Fig 5. Technical Steps to Segment Ablation Needles, Extract Needle Orientations and Tip Locations and Predict Ablation Zone

Evaluation and Experimental Setup

1. Needle segmentation algorithm evaluation using medical images

Medical images for testing are provided by Dr. Sheng Xu from the NIH Center of Interventional Oncology. The ground truth tip location and orientation of the acquired images are obtained by marking the endpoints of the ablation needles manually with MATLAB interface support. The corresponding angles and tip locations are computed from the two endpoints and served as the ground truth reference for testing.

Next, the automatic segmentation algorithm is applied to the unmodified image and the results (locations and directions) are compared to the ground truth. The tip location deviation is evaluated using mean square error and then converted to absolute distance unit using image resolution. The angle deviation is determined using **Equation 2** [6]. The resulting deviations are subsequently statistically analyzed for n=8 needles and are presented as Mean \pm Standard Error.

$$\cos(\beta) = \frac{|b_{dx}b_{sx} + b_{dy}b_{sy} + b_{dz}b_{sz}|}{\sqrt{b_{dx}^2 + b_{dy}^2 + b_{dz}^2} \cdot \sqrt{b_{sx}^2 + b_{sy}^2 + b_{sz}^2}} \quad \text{(Equation 2)}$$

$[b_{dx}b_{dy}b_{dz}]$ is the x, y, z directions of the predicted needle orientation, $[b_{sx}b_{sy}b_{sz}]$ is the x, y, z directions of the ground truth needle orientation, and β is the angle discrepancy between two vectors.

The predicted ablation zone for each medical image is generated and overlaid on the thresholded image for visualization. The selected ellipsoid for visualization has a long axis of 3.6 cm and a short axis of 2.6 cm.

2. Ablation zone prediction demonstration with thermochromic phantom and *ex vivo* experiments

MWA experiments are performed on tissue-mimicking thermochromic phantom [8] and *ex vivo* bovine liver at the NIH Clinical Center. The experiment utilized a Certus^{LK} LK15 Single Probe with varying settings.

2A. Tissue-mimicking Thermochromic Phantom

The thermochromic phantom changes color from light yellow to bright pink when coming in contact with high temperature. Multiple ablation settings are evaluated for their ablation zone appearance. The experiment was performed by varying the power setting between 40 W and 90 W for a 5-minute ablation duration each. The phantom, however,

cannot be CT imaged. Thus, the use of phantom is mainly for the visualization of the ablation zone to evaluate the realisticness of the ellipsoid model.

2B. Ex vivo Bovine Liver

Metal beads are placed inside the bovine liver to serve as tumor markers. A preoperative CT image is acquired to determine the target location. The ablation needle is guided using intraoperative CT images such that the bead is within the ablation range of the needle. Intraoperative images will be processed using the current algorithm, which would predict an ablation zone based on the needle's location and orientation. Using the preoperative CT scan, a virtual tumor of varying sizes (10 mm, 15 mm, and 20 mm in diameter) is generated using the bead location as the tumor centroid. The generated ablation volume is compared with the tumor volume to identify the efficacy of the treatment.

Results

1. Algorithm Performance With Medical Images

The accuracy of the extracted needle orientation and tip location is evaluated for all of the analyzed CT images. The algorithm achieved an accuracy of below 1 mm for needle tip localization. Specifically, a distance discrepancy of 0.82 ± 0.59 mm was achieved by comparing the segmented needle tip location to the ground truth. For needle orientation, the algorithm was able to determine the needle's orientation within 1° of accuracy. Specifically, an angle discrepancy of $0.74^\circ \pm 0.19^\circ$ was achieved when compared to the ground truth (**Figure 6**). The runtime of the algorithm is highly dependent on the size of the image. On average, the algorithm takes around **20 seconds** to process and display a medical image on a single CPU. For smaller single needle images, the runtime is roughly 12 seconds, while for multiple needle images, the runtime is around 30 seconds.

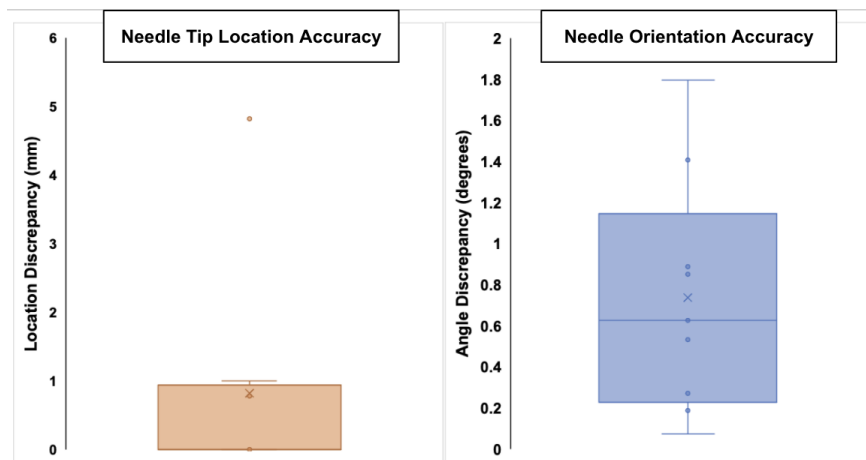


Fig 6. The algorithm accuracy for needle tip localization and needle orientation extraction

Visualization for the segmentation process for single needle and multiple needle processing is presented in **Figure 7A** and **7B** respectively. After preprocessing, connected component analysis, and object filtering, the needles are successfully segmented from other objects, including bright metal objects, bone fragments, and metal wires. Using the extracted feature from the segmented section, the ablation zone is approximated as an ellipsoid with specified dimensions, taking into account image spatial resolution.

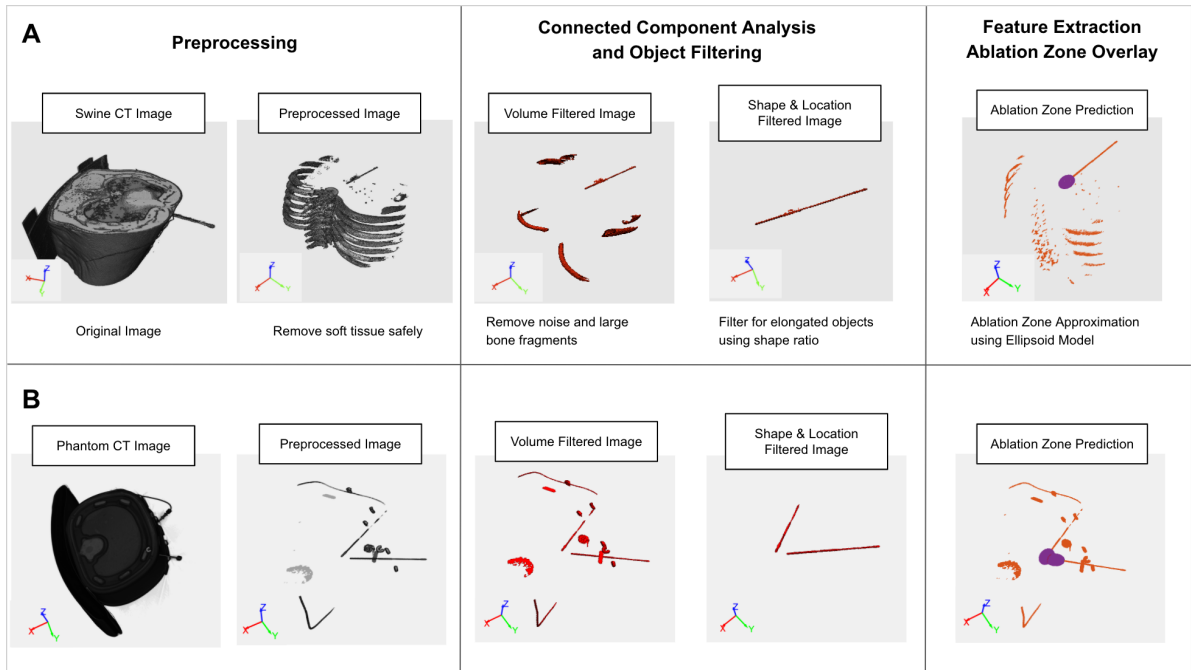


Fig 7. Visualization of the Needle Segmentation and Ablation Zone Prediction for **(A)** Single Ablation Needle in Swine CT Image and **(B)** Multiple Needles in Phantom CT Image. The ablation zone is presented in purple.

2. Ablation Zone Evaluation With Tissue-mimicking Thermochromic Phantom

The ablation zone result using thermochromic phantom is presented in **Figure 8**. The ablation zone as the result of the 90 W power setting is significantly larger than that of the 40 W power setting. The pink area closely resembles an ellipsoidal shape, further support the approximation of the ablation zone as an ellipsoid. Measurements of the ablation zone on the phantom showed a long axis of 3.2 cm and a short axis of 2.1 cm for the 40 W power setting. The technical specification provided by the manufacturer stated this number is 3.6 cm and 2.6 respectively, implying a somewhat overestimation of the actual zone. Similarly, for the 90 W power setting, the measurements showed an approximate 5.5 cm long axis and 1.9 cm short axis, smaller than the specification of 5.5 cm long axis and 3.6 cm short axis. However, it is important to note that the density and conductivity of the phantom material, as well as the experiment condition, are not

completely identical to that of liver tissue. Moreover, due to the small number of trials, this experiment cannot imply statistically significant observation. However, it presents a clear potential discrepancy between technical specification and the actual ablation zone generated by the ablation needle when presented with different material and conditions, which might vary in the body. The experiment also provided a strong visualization to confirm the ellipsoidal shape of the ablation zone, which depends on the needle orientation, location, and settings of the ablation needle. Moving forward, the technical specification provided by the manufacturer will be used to approximate the ablation zone.

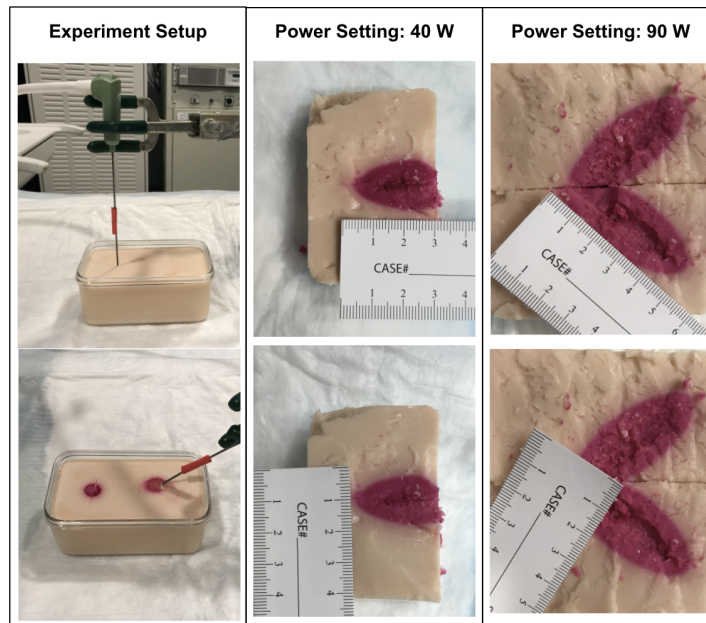


Fig 8. Ablation zone visualization using Tthermochromic phantom with varying power settings

3. Preliminary Integration of Ablation Zone Prediction Into Tumor Ablation Procedure

Before inserting the ablation needles, the metal beads are inserted into the bovine liver, from which a virtual tumor is generated with a diameter of 10 mm, 15 mm, or 20 mm. The preoperative image is taken and the virtual tumor is segmented, both presented in **Figure 10A**. In this case, the tumor is segmented from the preoperative image because it is generated from a planted bead. Ideally, the true location of the tumor would be determined from the intraoperative CT, not the preoperative scans.

Next, the ablation needles are inserted into the liver near the tumor site and the intraoperative CT scans are acquired. There are two sets of ablation images generated, one set with a single needle and one set with three needles. The algorithm is applied to the CT images and the resulting predicted ablation zone is presented in **Figure 9**.

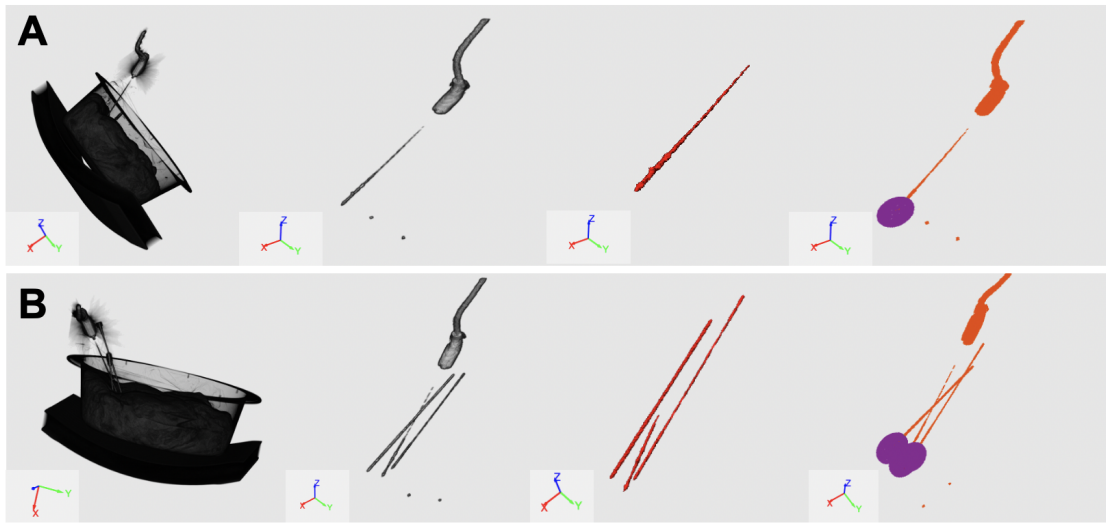


Fig 9. Ablation Zone Prediction for **(A)** Single Ablation Needle and **(B)** Multiple Needles in *ex vivo* bovine liver CT Images. The ablation zone is presented in purple.

This generated ablation zone is then overlaid onto the segmented tumor to evaluate for ablation location with respect to the tumor volume (**Figure 10B, 10C**). In this experiment, the needles are inserted too deep compared to the tumor site, leading to a poor overlap between the predicted ablation zone and the tumor volume. With this configuration of ablation needles, the larger tumors are ablated more as compared to small tumors. This presents a visualization example of the algorithm to help physicians navigate and approximate the span of the ablation zone.

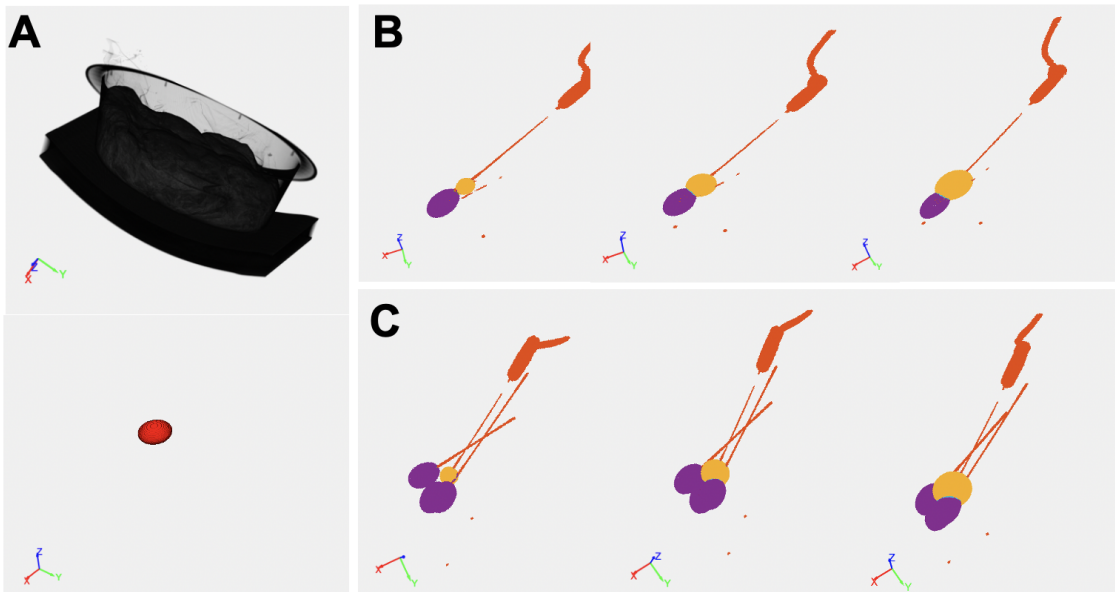


Fig 10. **(A)** The original preoperative CT scan (top) and the segmented virtual tumor using the planted metal bead (bottom) The ablation zone overlap onto the segmented tumor for **(A)** Single Ablation Needle and **(B)** Multiple Needles in *ex vivo* bovine liver CT Images. The tumor sizes are

10 mm, 15 mm, and 20 mm in diameter sequentially from left to right. The ablation zone is presented in purple. The tumor is presented in yellow.

Discussion

The segmentation algorithm performed well in general and obtained a high accuracy for needle orientation and tip location identification. There are, however, occasional failures with cases where multiple needles are attached to one another and the 3D Hough Transform could not resolve them effectively. The algorithms also involved a lot of hyperparameters that need to be fine-tuned and may be sensitive to outlier cases.

The evaluation of ablation zone prediction accuracy is still very difficult due to the lack of intraoperative visualization of the ablation zone. The approximation of the ablation zone using an ellipsoid model is standard but also inaccurate due to multiple variations involved in the generation of the ablation zone, namely tissue properties such as thermal/electrical conductivity and density, or the heat sink effects caused by major blood vessels. To improve ablation zone approximation accuracy, some of these parameters need to be taken into consideration to modify the existing ellipsoid model.

The generated ablation zone is a preliminary version that currently serves a visualization purpose. Looking forward, the algorithm should be further optimized to increase generalizability. Further testings and evaluations should be done on a large dataset of patient images. Ablation zone approximation accuracy can be evaluated using CT-imagable tissue-mimicking thermochromic phantoms. Next, more clinically meaningful information can be computed and extracted from the current algorithm, such as percentages of tumor volume ablated/remaining or the relative distance and orientation between the needle tip location and the tumor location. Improving visualization and incorporating an intuitive user interface will also provide can help push the effort to integrate the result into a clinical setting.

Progress Evaluation

Overall, the project went as planned with no major drawbacks. Some modifications to the maximum deliverables and dependencies are made to match the circumstances and feasibility of the project.

1. Dependencies

Most of the dependencies of the project are resolved by the expected deadlines. However, due to the administrative and paperwork difficulties, NIH badge access and clinical data transfer agreement could not be completed. Instead, the algorithm was developed mainly using phantom and ex vivo images. The list of dependencies and their details are listed in **Table 1**.

Table 2. Details and status associated with project dependencies

Dependency	Reasoning	Personnel	Current Status	Completion Date	
Access to internet and MATLAB, and other softwares	Crucial for research, code implementation and communications	N/A	Continuous access through JHU secured	N/A	✓
Image Conversion to Nifti File	Simplify the image preprocessing process	Dr. Xu	Completed for obtained images	03/15	✓
Ground Truth for Medical Images	Reference for testing, crucial to evaluate algorithm performance	Dr. Xu and Dr. Wood	Completed for obtained images	03/20	✓
Medical Images	Crucial for algorithm development and testing	Dr. Xu and Dr. Wood	Obtained phantom images	03/20	✓
Clinical Data Transfer Agreement	Access to patient medical images	NIH admin, Dr. Xu	Work with phantom/swine images and modified medical images Instead	03/24	✗
Phantom and ex vivo samples, experiment space and instrument	Evaluate ablation zone prediction algorithm	Dr. Xu and Dr. Wood	Completed	04/31	✓

2. Key Activities and Deliverables

The key activities and deliverables for this project, along with their completion status are listed in **Table 2** and are categorized into the minimum, expected, and maximum activities and corresponding deliverables. Overall, this project has completed the minimum and expected deliverables and part of the maximum deliverables. To evaluate the accuracy of the predicted ablation zone, a CT-imagable tissue-mimicking thermo-chromic phantom will be needed.

Table 2. The key activities and corresponding deliverables. Green sections are completed, yellow sections are partially completed, and red sections are not completed.

	Activity	Deliverable
Minimum	<ul style="list-style-type: none"> MATLAB implementation to process and standardize Nifti CT images Segment ablation needles from background 	<ul style="list-style-type: none"> MATLAB program and documentation on how to implement the code
Expected	<ul style="list-style-type: none"> Extract needle tip location and needle orientation Evaluate algorithm accuracy using manually labeled medical images 	<ul style="list-style-type: none"> MATLAB code and documentation Manually labeled CT images Reports on algorithm performance with graphs and statistical analysis
Maximum	<ul style="list-style-type: none"> Superimpose colorized isotherms using FEA ellipsoid model to predict the ablation zone Evaluate prediction accuracy with phantom/ex vivo experiments 	<ul style="list-style-type: none"> MATLAB code and documentation Ablation zone visualization Reports on ablation zone accuracy performance with graphs and statistical analysis

3. Schedule Adherence

The timeline for the project was followed pretty closely with a couple of modifications due to the change of dependencies and deliverables. The updated timeline of the semester is presented in **Figure 11**.

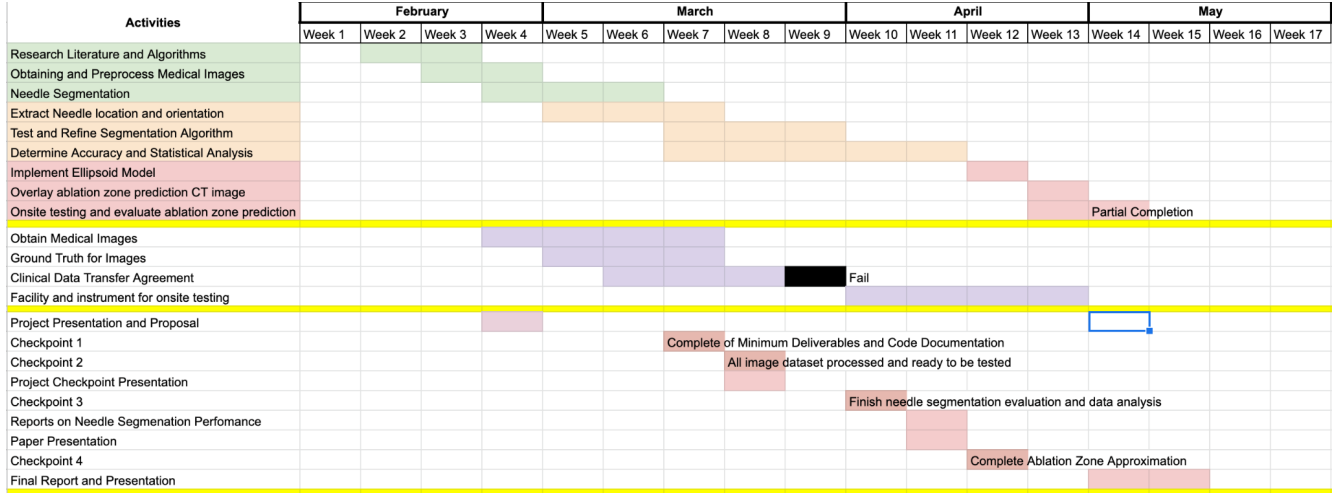


Fig 11. Timeline for the project implementation, resolving dependencies, and fulfilling class requirements

Final Remarks

The project result is a preliminary effort to help physicians visualize the ablation zone intraoperatively and better navigate the tumor ablation procedure. The performance of the algorithm is promising and if optimized, can reach greater generalizability. Future improvements of the algorithm and thorough evaluation can provide a more comprehensive view of the clinical usability of the algorithm. Personally, the project was a great learning and technical development opportunity for me.

Special appreciation to the project mentors and course advisors for their support:

Dr. Sheng Xu (xus2@cc.nih.gov)

Dr. Michael Kassin (michael.kassin@nih.gov)

Dr. Bradford J. Wood (bwood@cc.nih.gov)

The NIH Center for Interventional Oncology, Interventional Radiology

Dr. Russell Taylor (rht@jhu.edu)

Max Zhaoshuo Li (zli122@jhu.edu)

Johns Hopkins Whiting School of Engineering

References

- [1] (ACR), Radiological. "Radiofrequency Ablation (RFA) | Microwave Ablation (MWA) - Liver Tumors". *Radiologyinfo.Org*, 2019, <https://www.radiologyinfo.org/en/info.cfm?pg=rfaliver>.
- [2] "Radiofrequency Ablation For Cancer - Mayo Clinic". *Mayoclinic.Org*, 2018, <https://www.mayoclinic.org/tests-procedures/radiofrequency-ablation/about/pac-20385270>.
- [3] Egger, Jan et al. "Interactive Volumetry Of Liver Ablation Zones." *Scientific reports* vol. 5 15373. 20 Oct. 2015, doi:10.1038/srep15373
- [4] Santos, Ricardo S. et al. "Electromagnetic Navigation To Aid Radiofrequency Ablation And Biopsy Of Lung Tumors". *The Annals Of Thoracic Surgery*, vol 89, no. 1, 2010, pp. 265-268. *Elsevier BV*, doi:10.1016/j.athoracsur.2009.06.006. Accessed 25 Feb 2021.
- [5] Amalou, H., Wood, B.J. Electromagnetic tracking navigation to guide radiofrequency ablation of a lung tumor. *J Bronchology Interv Pulmonol.* 2012;19(4):323-327. doi:10.1097/LBR.0b013e31827157c9
- [6] Zhou, H., Qiu, W., Ding, M., and Zhang, S., "Automatic needle segmentation in 3D ultrasound images using 3D improved Hough transform", in *Medical Imaging 2008: Visualization, Image-Guided Procedures, and Modeling*, 2008, vol. 6918. doi:10.1117/12.770077.
- [7] Alpers, J., Hansen, C., Ringe, K., & Rieder, C. "CT-Based Navigation Guidance for Liver Tumor Ablation". In *Eurographics Workshop on Visual Computing for Biology and Medicine*. The Eurographics Association. 2017
- [8] Mikhail, A. S., Negussie, A. H., Graham, C., Mathew, M., Wood, B. J., & Partanen, A. (2016). Evaluation of a tissue-mimicking thermochromic phantom for radiofrequency ablation. *Medical physics*, 43(7), 4304. <https://doi.org/10.1118/1.4953394>
- [9] Wood B.J., Locklin J.K., Viswanathan A, et al. Technologies for guidance of radiofrequency ablation in the multimodality interventional suite of the future. *J Vasc Interv Radiol.* 2007;18(1 Pt 1):9-24. doi:10.1016/j.jvir.2006.10.013
- [10] Zhang, J., Chauhan, S. Real-time computation of bio-heat transfer in the fast explicit dynamics finite element algorithm (FED-FEM) framework, *Numerical Heat Transfer, Part B: Fundamentals*. 2019; 75:4, 217-238, DOI: [10.1080/10407790.2019.1627812](https://doi.org/10.1080/10407790.2019.1627812)

Appendix 1: Code Documentation

The MATLAB code for the project can be found [here](#).

The program requires the latest version of MATLAB (2021a) to run without error and the installation of the Computer Vision Toolbox.

Only the first file **AblationZonePrediction.m** is needed to be run.

1. AblationZonePrediction.m

The main file that executes the program.

Inputs: image filename, whether multiple needles are expected, and the long axis and short axis of the ellipsoid representing the ablation zone.

Outputs: Print out the needle orientation and tip location of each needle in the image sequentially, display the volume visualization of the different stages in the algorithm.

This file call *ExtractOrientationAndTipLocation.m* and *PredictAblation.m*.

2. ExtractOrientationAndTipLocation.m

This function computes the needle orientation and needle tip location using PCA.

Inputs: CC: connected component object; BW: the binary volume image; needle: the index of needle-like connected components in CC; multiple_needles: boolean (1 if multiple needles are expected and 0 otherwise)

Outputs: NeedleFeatures: A vector containing needle tip location and needle orientation of all needle objects.

This function calls *Hough3DLineDetection.m*.

3. Hough3DLineDetection.m

This function is used to identify line segments in 3D from a collection of voxels.

Inputs: voxels: the coordinates of all the voxels in CT image coordinate; boundingbox: the bounding box of the object, formatted as a 6x1 matrix specified in MATLAB `bwconncomp3` function; imgsize: the size of the original image; d_ang: angle resolution of interest, rho_num: the size of the 4th dimension of the Hough voting matrix that determines the distance resolution.

Outputs: Hough: The 4D Hough voting matrix; VoxList: the list of the Hough coordinates that each voxel voted for.

4. PredictAblation.m

This function is used to generate an ellipsoid ablation zone based on the technical specification.

Inputs: Vol: the original 3D volume; tip: the location of the needle tip; direction: the unit vector indicating the orientation of the ablation needle; long_axis: the size of the long axis of the ellipsoid model (millimeter); short_axis: the size of the short axis of the ellipsoid model (millimeter); resolution: the pixel dimension of the image.

Outputs: ablation: The 3D image of an ellipsoid that approximates the ablation zone.